

SUPPORTING INFORMATION

Pharmaceuticals removal in different water matrixes by Fenton process at near neutral pH: Dohelert design and transformation products identification by UHPLC-QTOF MS using purpose-built database

E. Cuervo Lumbaque^a, R. M. Cardoso^a, A. Dallegrave^a, L. O. dos Santos^a, M. Ibáñez^b,
F. Hernández^b, C. Sirtori^{a*}

^a Instituto de Química - Universidade Federal do Rio Grande do Sul, Av. Bento Gonçalves, 9500, Porto Alegre-RS, Brazil.

^b Research Institute for Pesticides and Water, University Jaume I, Castellón 12071, Spain.

*Corresponding author

E-mail address: carla.sirtori@ufrgs.br

-S.1 Doehlert matrix – optimization and response surface results

Table S.1.1 Selected parameters for ANOVA.

ANOVA parameters	
parameters (p)	10
Total analysis (n)	16
Levels (m)	13
Level of significance (α)	0.05

Table S.1.2 Analysis of variance of the Doehlert design executed in the study to optimize experimental conditions in Fenton process, at the significance level of 0.05.

Variance analysis					
VS	QS	DF	QM	Fcalc.	<i>p</i>
Regression	804.6	9	89.397	5.1812*	0.0291
Residuals	103.5	6	17.254		
Lack of fit	91.77	3	30.589	7.8051	0.0627
Pure error	11.76	3	3.9191		
Total	908.1	15			
% variance explained				88.6	
% maximum variance explainable				98.705	

* The significant values are presented in bold; VS: variance source, QS: quadratic sums, DF: degrees of freedom, QA: quadratic mean, Fcalc: calculated value of measured test F, p: statistical parameter p.

Figure S.1.1 Normal probability graph of the variables investigated utilizing the Doehlert design in Fenton process optimization.

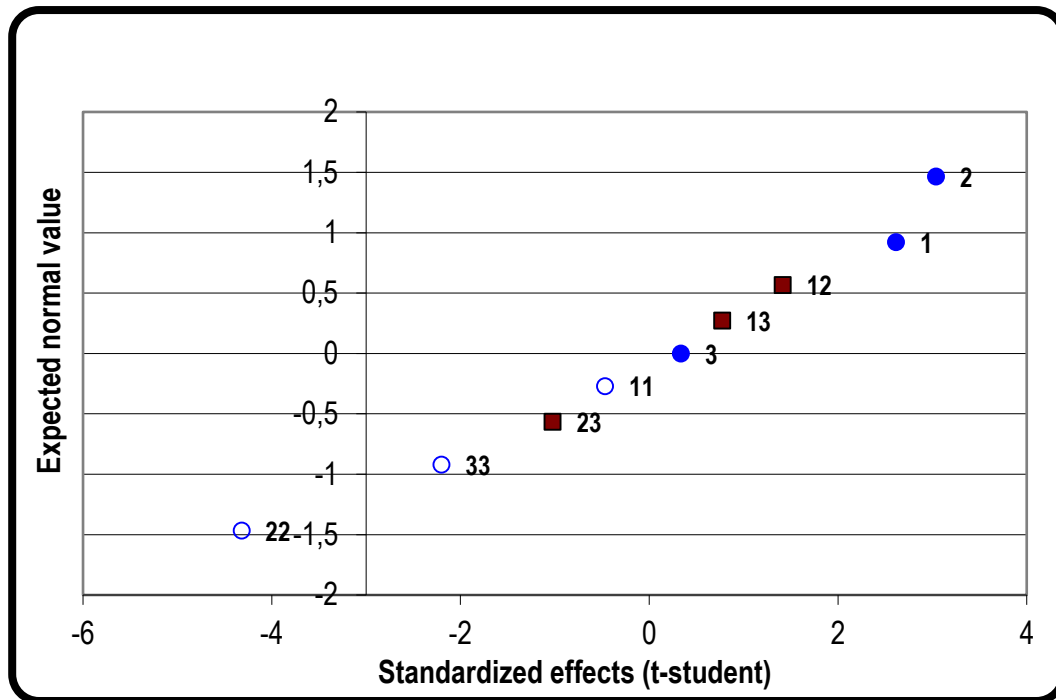
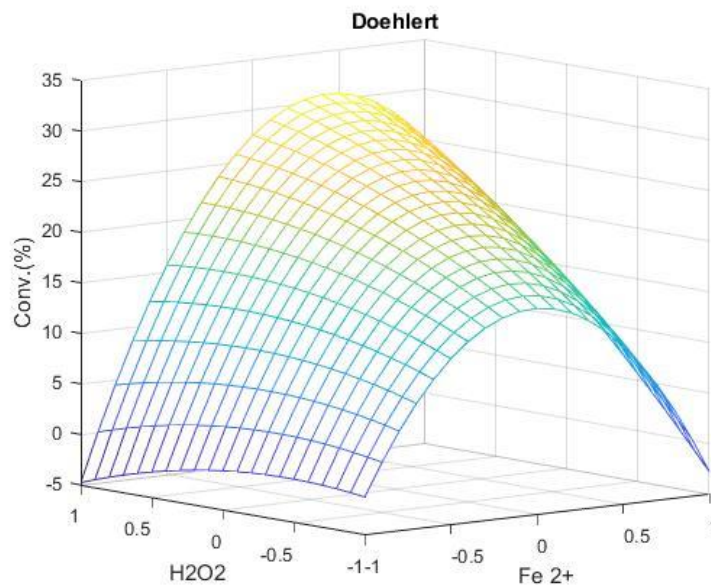


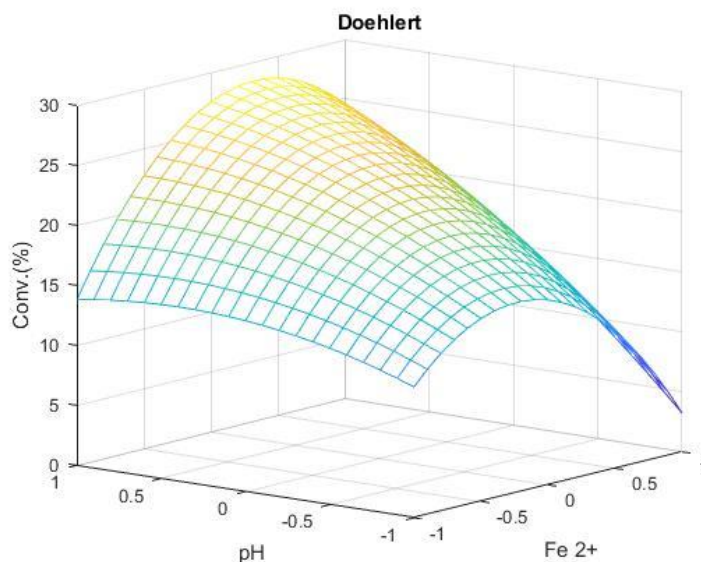
Figure S.1.2 Response surface of the Doehlert design for two variables: H₂O₂ and Fe²⁺.



$$R(i,j) = (11.22) + (6.342) * (x(i)) + (7.383521916) * (y(j)) + (6.708595388) * (x(i)^2) + (-$$

$$9.469458407*(y(j)^2)+(7.928207959)*((x(i))*(y(j))) \quad \text{Equation (i)}$$

Figure S.1.3 Response surface of the Doehlert design for two variables: pH and Fe²⁺.



$$R(i,j) = (11.22) + (6.342)*(x(i)) + (0.788176186)*(y(j)) + (6.708595388)*(x(i)^2) + (-0.014800799)*(y(j)^2) + (4.829431058)*((x(i))*(y(j))) \quad \text{Equation (ii)}$$

S.2 Homemade database used for automated identification of some pharmaceuticals transformation products (TPs) generated during Fenton process

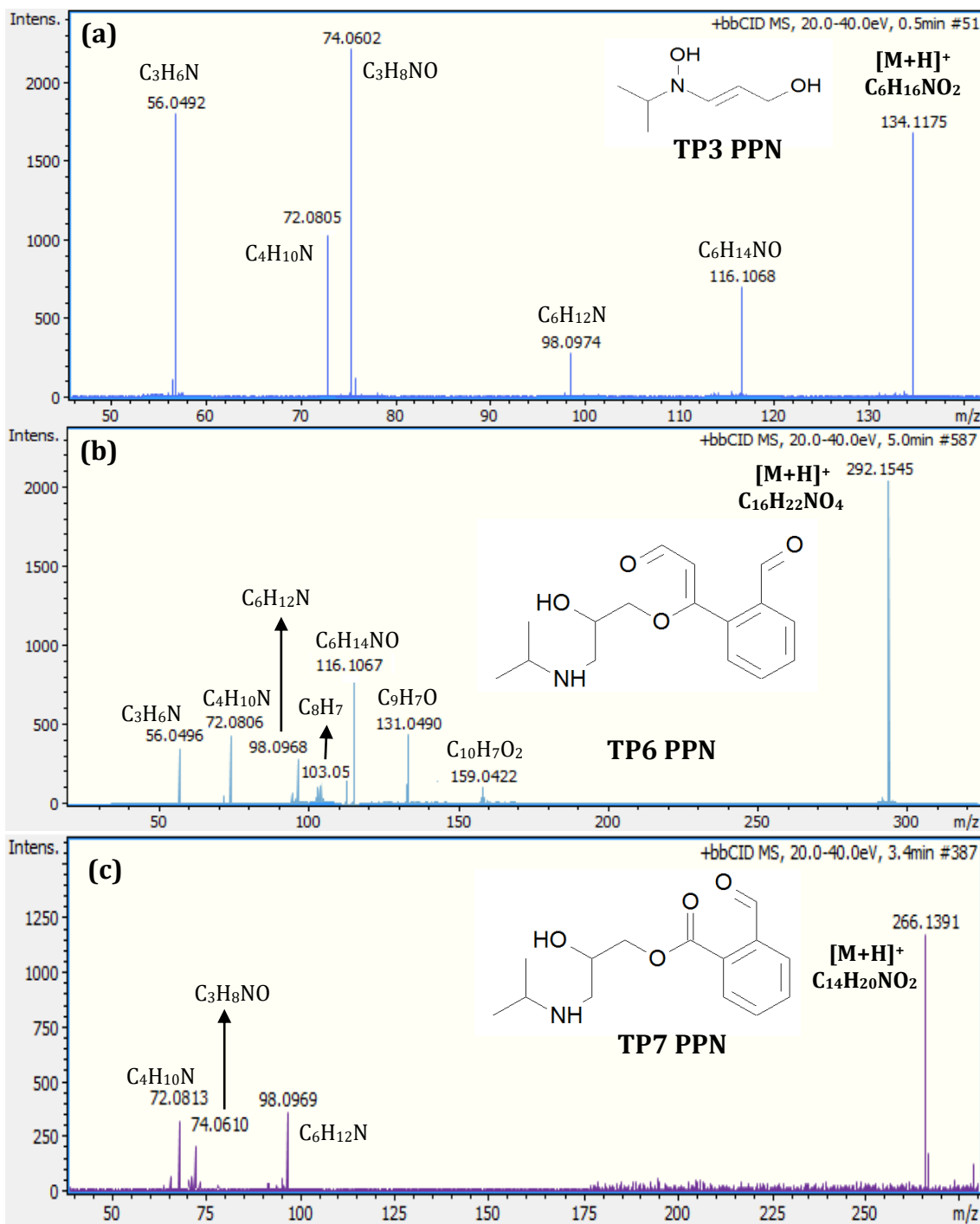
Table S.2.1 TPs monitored by automated screening during Fenton process.

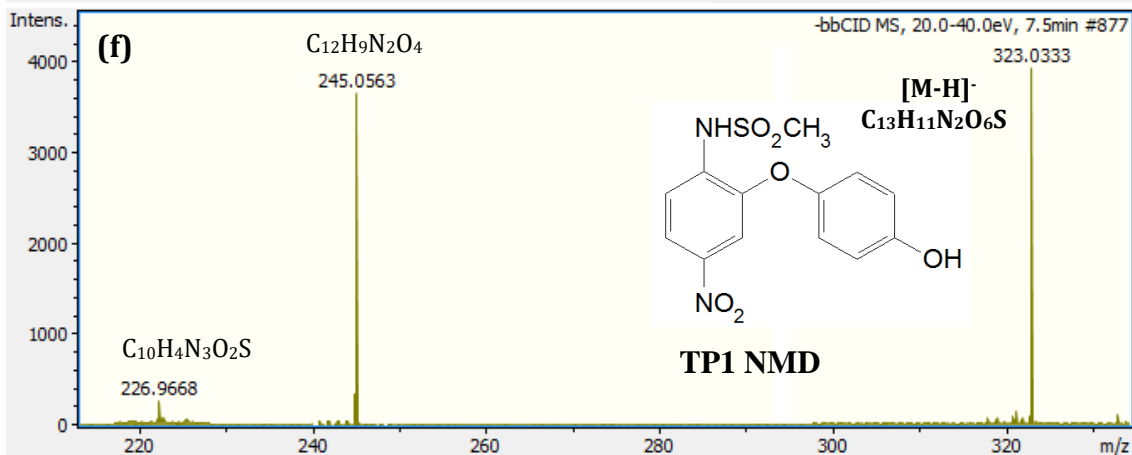
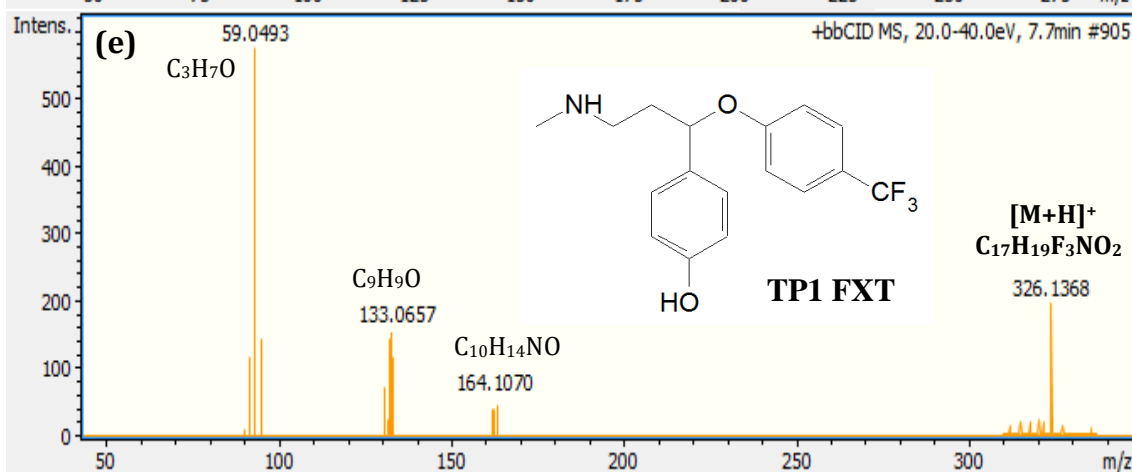
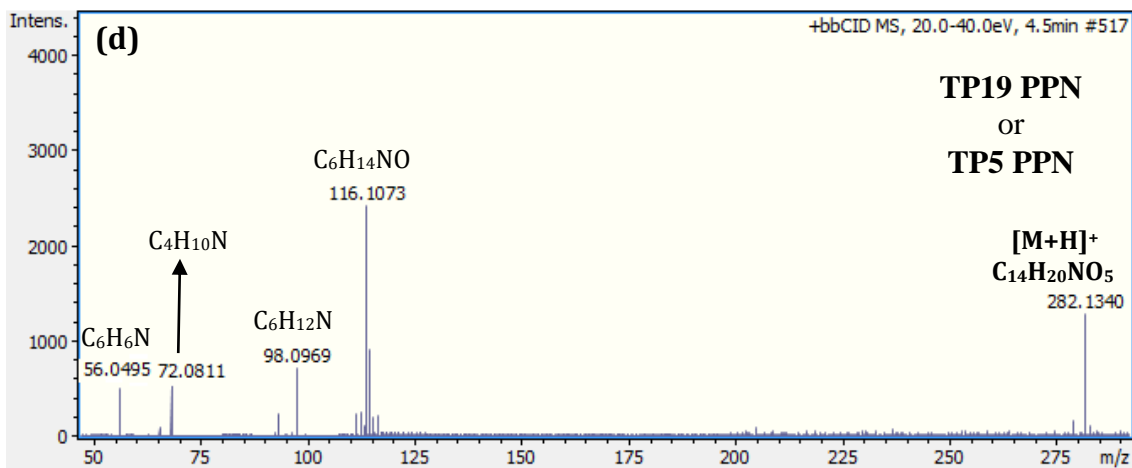
Compound	Elemental Composition	Ion Mass [M+H] ⁺ or [M-H] ⁻	Reference
TP1 PPN	C ₅ H ₁₁ NO ₂	118.0863	[1]
TP2 PPN	C ₆ H ₁₃ NO ₂	132.1019	[1]
TP3 PPN	C ₆ H ₁₅ NO ₂	134.1176	[1]
TP4 PPN	C ₆ H ₁₅ NO ₃	150.1125	[1]
TP5 PPN	C ₁₄ H ₁₉ NO ₅	282.1336	[1]
TP6 PPN	C ₁₆ H ₂₁ NO ₄	292.1543	[1]
TP7 PPN	C ₁₄ H ₁₉ NO ₄	266.1387	[1]
TP8 PPN	C ₁₄ H ₁₃ NO ₄	164.0917	[1]

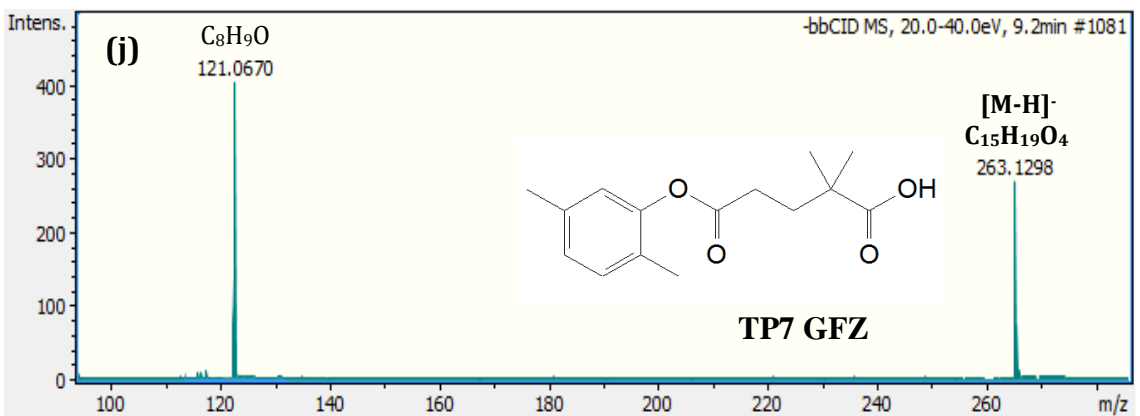
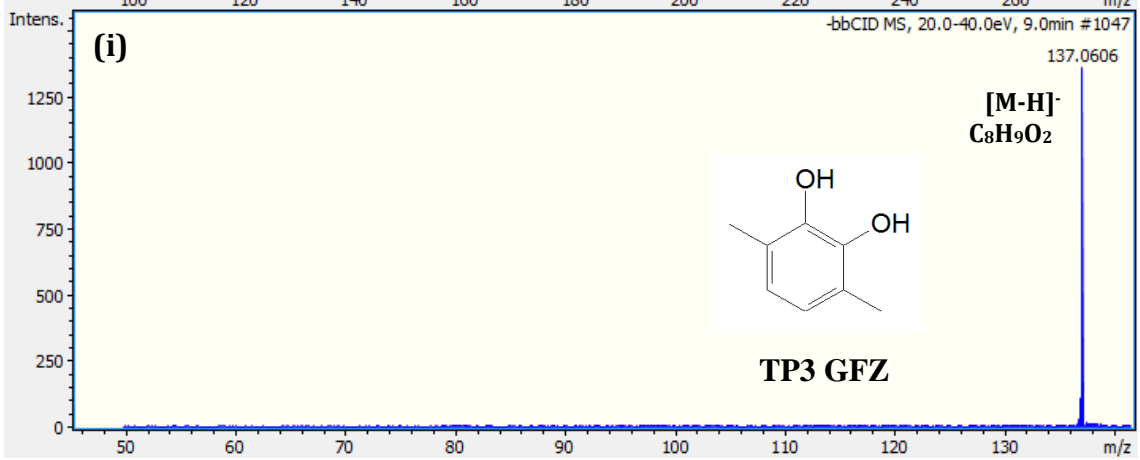
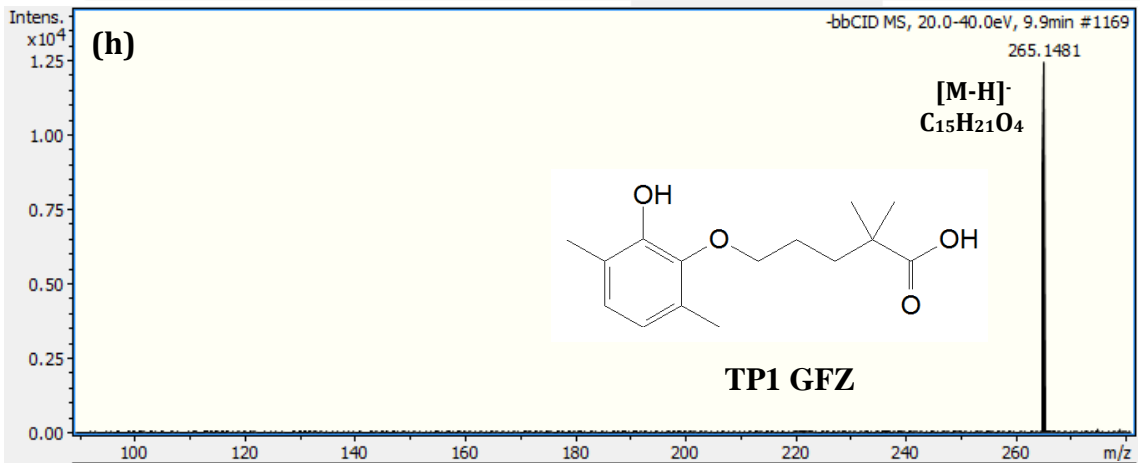
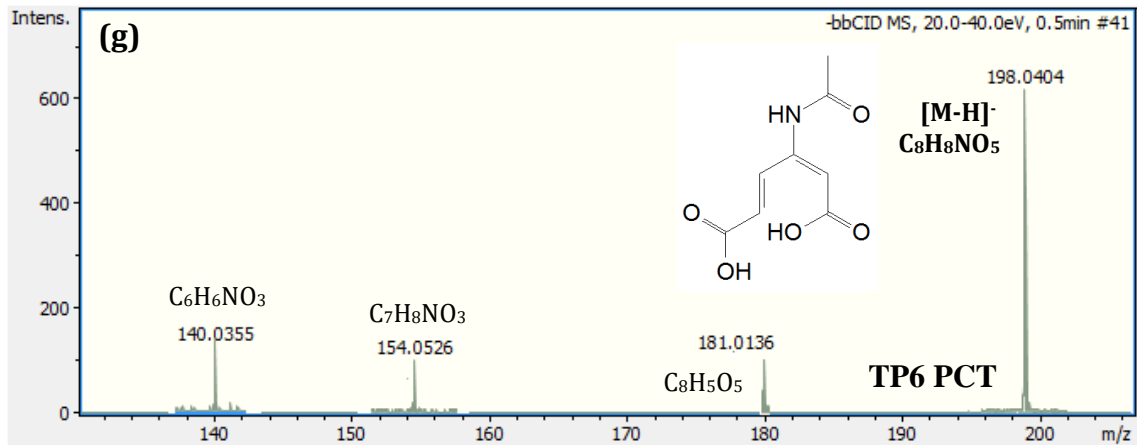
TP9 PPN	C16H19NO3	274.1438	[1]
TP10 PPN	C16H19NO3	274.1438	[1]
TP11 PPN	C16H19NO3	274.1438	[1]
TP12 PPN	C16H21NO3	276.1594	[1]
TP13 PPN	C16H21NO3	276.1594	[1]
TP14 PPN	C16H21NO3	276.1594	[1]
TP15 PPN	C16H21NO3	276.1594	[1]
TP16 PPN	C16H21NO3	276.1594	[1]
TP17 PPN	C16H21NO3	276.1594	[1]
TP18 PPN	C14H19NO5	282.1336	[1]
TP19 PPN	C14H19NO5	282.1336	[1]
TP20 PPN	C14H19NO5	282.1336	[1]
TP21 PPN	C16H21NO4	292.1543	[1]
TP22 PPN	C16H21NO4	292.1543	[1]
TP23 PPN	C16H21NO4	292.1543	[1]
TP24 PPN	C16H21NO4	292.1543	[1]
TP25 PPN	C16H23NO4	294.1700	[1]
TP26 PPN	C16H21NO5	308.1492	[1]
TP27 PPN	C16H21NO5	308.1492	[1]
TP28 PPN	C16H23NO5	310.1649	[1]
TP29 PPN	C16H23NO5	310.1649	[1]
TP30 PPN	C16H23NO5	310.1649	[1]
TP31 PPN	C16H23NO5	310.1649	[1]
<hr/>			
TP1 DIP	C6H4N	105.0447	[2]
TP2 DIP	C11H14N2O3	223.1077	[2]
TP3 DIP	C11H12N2O3	221.092	[2]
TP4 DIP	C8H10N2O	151.0865	[2]
TP5 DIP	C10H11NO4	210.076	[2]
TP6 DIP	C10H9NO3	192.0655	[2]
TP7 DIP	C12H15N3O3	250.1186	[2]
TP8 DIP	C8H9NO	136.0756	[2]
TP9 DIP	C11H12N2O2	205.0971	[2]
TP10 DIP	C9H12N2O	165.1022	[2]
TP11 DIP	C11H12N2O	189.1022	[2]
TP12 DIP	C11H13N3O	204.113	[3]
TP13 DIP	C12H15N3O3	250.118	[3]
TP14 DIP	C11H12N2O3	221.0918	[3]
TP15 DIP	C12H15N3O	218.1287	[3]
TP16 DIP	C6H7N	94.0652	[3]
TP17 DIP	C12H13N3O2	232.1078	[3]
TP18 DIP	C9H10N2O3	195.0759	[3]
<hr/>			
TP1 PCT	C2H5NO	60.0443	[4]
TP2 PCT	C6H5NO3	140.0342	[4], [5]
TP3 PCT	C8H9NO4	184.0604	[4]
TP4 PCT	C8H9NO3	168.0655	[5]
TP5 PCT	C8H9NO3	168.0655	[4], [5], [6]

TP6 PCT	C8H9NO5	200.0559*	[5], [6]
TP7 PCT	C8H7NO2	150.0555*	[5]
TP8 PCT	C6H6O2	111.0446*	[5], [6]
TP9 PCT	C6H6O3	127.0395*	[5]
TP10 PCT	C6H4O2	109.0289*	[5]
TP11 PCT	C6H7NO	110.0605*	[5]
TP12 PCT	C6H5NO4	156.0297*	[5]
TP1 FRS	C12H11N2ClSO6	347.0104*	[7]
TP2 FRS	C12H11N2ClSO6	347.0104*	[7]
TP3 FRS	C12H9N2O5SCl	328.9999*	[7]
TP4 FRS	C12H9N2O5SCl	328.9999	[7]
TP5 FRS	C7H7N2O4SCl	250.9893	[7], [8], [9]
TP6 FRS	C14H14CIN3O4S2	388.0193*	[8]
TP7 FRS	C18H19CIN2O11S	507.0476*	[8]
TP8 FRS	C18H19CIN2O11S	507.0476*	[8]
TP9 FRS	C7H8CIN3O4S2	297.9723*	[8]
TP10 FRS	C12H10CIN2O6S	344.9948	[9]
TP11 FRS	C11H10CIN2O5S	317.9999	[9]
BTP1 GFZ	C15H20O5	279.1241	[10]
TP1 GFZ	C15H21O4	264.1361*	[11]
TP2 GFZ	C15H21O5	281.1389*	[11]
TP3 GFZ	C8H10O2	138.0681	[11]
TP4 GFZ	C15H21O5	281.1389*	[11]
TP5 GFZ	C15H19O6	295.1182*	[11]
TP6 GFZ	C15H19O4	263.1283*	[11]
TP7 GFZ	C15H20O4	264.1361*	[11]
TP8 GFZ	C9H9O3	165.0551*	[11]
TP1 FXT	C17H18F3NO2	326.13656	[12]
TP2 FXT	C17H18F3NO4	358.12882	[12]
TP3 FXT	C10H15NO	166.12383	[12]
TP4 FXT	C10H13NO	164.10826	[12]
TP5 FXT	C12H12F3NO2	260.09117	[12]
TP6 FXT	C9H10F3NO3	238.0705	[12]
TP7 FXT	C15H14F2O3	281.09959	[12]
TP8 FXT	C15H16F2O4	299.11021	[12]
TP9 FXT	C15H16F2O4	299.10973	[12]
TP1 NMD	C13H12N2O6S	323.033784	[13]
TP2 NMD	C16H18N2O5S	349.085820	[13]
TP3 NMD	C15H16N2O5S	335.070170	[13]
TP4 NMD	C13H12N2O10S2	418.985517	[13]
TP5 NMD	C13H14N2O3S	279.08034	[14]
TP6 NMD	C13H14N2O4S	295.075254	[14]
TP1 DZP	C14H12ClNO	246.0680	[15]
TP2 DZP	C16H14ClNO3	304.0735	[15]
TP3 DZP	C16H14ClNO3	304.0735	[15]
TP4 DZP	C16H11ClN2O2	299.0578	[15]

*TPs identified by LC-MS/MS.







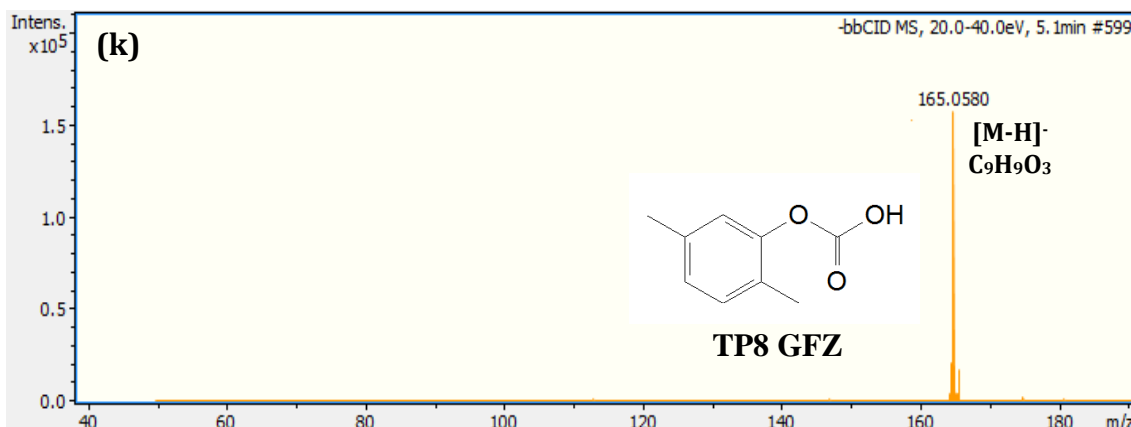


Figure S.2.1 MS spectra in bbCID mode using High Collision Energy for the TPs identified for: (a) (b) (c) and (d) propranolol, (e) fluoxetine, (f) nimesulide, (g) paracetamol, (h) (i) (j) and (k) gemfibrozil during Fenton process.

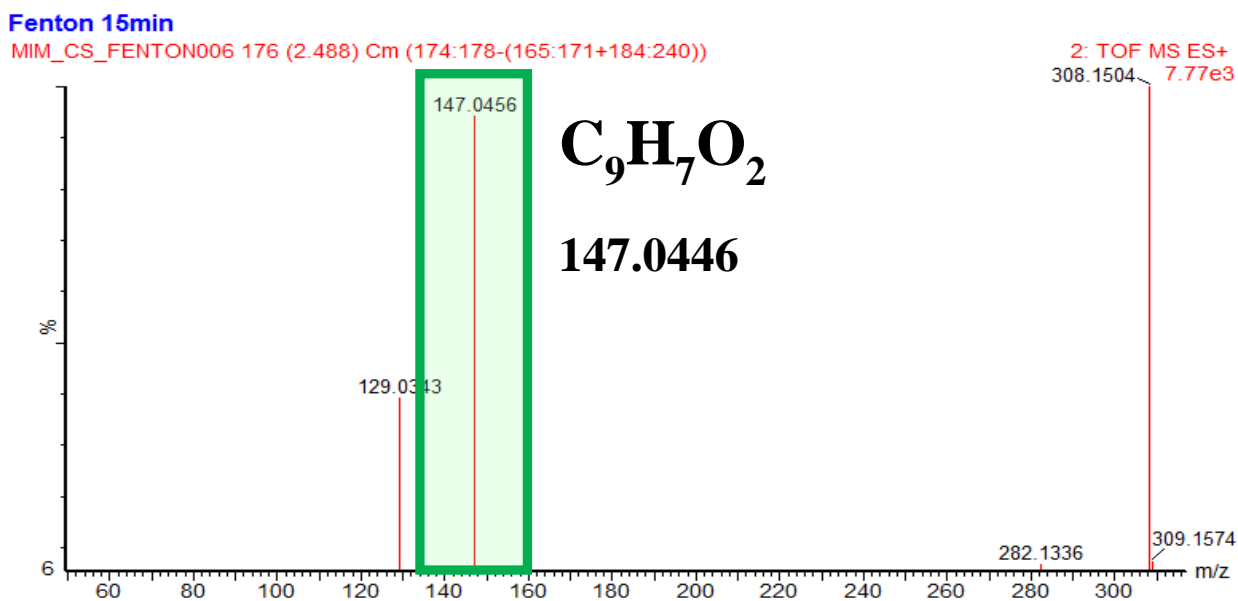


Figure S.2.2 TP26 PPN identified during Fenton degradation.

References

- [1] J. Santiago-Morales, A. Agüera, M. del M. Gómez, A. R. Fernández-Alba, J. Giménez, S. Esplugas, R. Rosal. Transformation products and reaction kinetics in simulated solar light photocatalytic degradation of propranolol using Ce-doped TiO₂. Appl. Catal. B Environ. 129 (2013) 13–29.

- [2] M. J. Gómez, C. Sirtori, M. Mezcuca, A. R. Fernández-Alba, A. Agüera. Photodegradation study of three dipyrone metabolites in various water systems: Identification and toxicity of their photodegradation products. *Water Res.* 42 (2008) 2698–2706.
- [3] L. A. Pérez-Estrada, S. Malato, A. Agüera, A. R. Fernández-Alba. Degradation of dipyrone and its main intermediates by solar AOPs. *Catal. Today* 129 (2007) 207–214.
- [4] A.G. Trovó, R. F. P. Nogueira, A. Agüera, A. R. Fernandez-Alba, S. Malato. Paracetamol degradation intermediates and toxicity during photo-Fenton treatment using different iron species. *Water Res.* 46 (2012) 5374-5380.
- [5] E. Moctezuma, E. Leyva, C. A. Aguilar, R. A. Luna, C. Montalvo. Photocatalytic degradation of paracetamol: Intermediates and total reaction mechanism. *J. Hazard. Mater.* 243 (2012) 130-138.
- [6] N. H. El Najjar, A. Touffet, M. Deborde, R. Journal, N. K. Vel Leitner. Kinetics of paracetamol oxidation by ozone and hydroxyl radicals, formation of transformation products and toxicity. *Sep. Purif. Technol.* 136 (2014) 137–143.
- [7] C. Laurencé, M. Rivard, I. Lachaise, J. Bensemoun, T. Martens. Preparative access to transformation products (TPs) of furosemide: a versatile application of anodic oxidation. *Tetrahedron* 67 (2011) 9518–9521.
- [8] M. Ibáñez, V. Borova, C. Boix, R. Aalizadeh, R. Bade, N.S. Thomaidis, F. Hernández. UHPLC-QTOF MS screening of pharmaceuticals and their metabolites in treated wastewater samples from Athens. *J. Hazard. Mater.* 323 (2017) 26–35.
- [9] C. Laurencé, M. Rivard, T. Martens, C. Morin, D. Buisson, S. Bourcier, M. Sablierd, M. A. Oturan. Anticipating the Fate and Impact of Organic

- Environmental Contaminants: a New Approach Applied to the Pharmaceutical Furosemide. *Chemosphere* 113 (2014) 193–199.
- [10] C. Boix, M. Ibañez, J. V. Sancho, J. R. Parsons, P. de Voogt, F. Hernández. Biotransformation of pharmaceuticals in surface water and during waste water treatment: Identification and occurrence of transformation products. *J. Hazard. Mater.* 302 (2016) 175-185.
- [11] P. Chen, F. Wang, Z.-F. Chen, Q. Zhang, Y. Su, L. Shen, K. Yao, Y. Liu, Z. Cai, W. Lv, G. Liu. Study on the photocatalytic mechanism and detoxicity of gemfibrozil by a sunlight-driven TiO₂/carbon dots photocatalyst: The significant roles of reactive oxygen species. *Appl. Catal. B Environ.* 204 (2017) 250–259.
- [12] Y. Zhao, G. Yu, S. Chen, S. Zhang, B. Wang, J. Huang, S. Deng, Y. Wang. Ozonation of antidepressant fluoxetine and its metabolite product norfluoxetine: Kinetics, intermediates and toxicity. *Chem. Eng. J.* 316 (2017) 951–963.
- [13] X. Sun, K-L. Xue, X-Y. Jiao, Q. Chen, L. Xu, H. Zheng, Y-F. Ding. Simultaneous determination of nimesulide and its four possible metabolites in human plasma by LC–MS/MS and its application in a study of pharmacokinetics. *J. Chromatography B* 1027 (2016) 139-148.
- [14] M. Carini, G. Aldini, R. Stefani, C. Marinello, R. M. Facino. Mass spectrometric characterization and HPLC determination of the main urinary metabolites of nimesulide in man. *J. Pharm. Biomed. Anal.* 18 (1998) 201-211.
- [15] I. Carpinteiro, R. Rodil, J. B. Quintana, R. Cela. Reaction of diazepam and related benzodiazepines with chlorine. Kinetics, transformation products and *in-silico* toxicological assessment. *Water Res.* 120 (2017) 280-289.